Applied Energy 402 (2026) 127038

Contents lists available at ScienceDirect

Applied Energy

journal homepage: www.elsevier.com/locate/apen

A demand-side optimisation framework for assessing energy flexibility potential of integrated energy systems in building complex

Annalisa Bringiotti [a,b], Fabiano Pallonetto [b,c], Mattia De Rosa [a,d,*]

[a] Dipartimento di Ingegneria Meccanica, Energetica, Gestionale e dei Trasporti (DIME). Università degli Studi di Genova, Via All'Opera Pia 15/A, 16145 Genoa, Genoa, Italy

[b] International Renewables and Energy Systems Integration (IRESI), School of Business, National University of Ireland Maynooth, Co. Kildare, Ireland

[c] School of Business, National University of Ireland Maynooth (NUIM), Maynooth, W23 F2H6, Co. Kildare, Ireland

[d] International Centre of Energy Resource Management (iCERM). Genoa Division, Genoa, Italy

HIGHLIGHTS

- Smart management systems can optimise costs and unlock building energy flexibility.
- Flexibility potential and its marginal cost can be assessed at aggregated level.
- Access to real-time pricing unlocks highest flexibility potential.
- Optimal sizing of thermal storage can be determined.

ARTICLE INFO

Keywords:
Energy flexibility
Demand side management
Demand response
Energy systems
Flexibility market
Smart control
Building energy modelling
Techno-economic assessment

ABSTRACT

This study presents an energy management system for residential buildings based on advanced demand-side management strategies that can assess building energy flexibility potential. A case study of a Dublin-based condominium equipped with a hybrid energy system – consisting of a heat pump, gas boiler, solar photovoltaic panels, and thermal energy storage – is investigated. The optimisation algorithm adjusts the energy system schedule to minimise daily operational costs while meeting thermal and electrical demands. Demand response actions are introduced and evaluated in terms of energy flexibility potential and marginal cost. Simulations for a typical winter week indicate that triggering demand response actions leads to increased operational costs, which can be interpreted as the cost of flexibility – a key parameter for shaping flexibility markets. Additionally, the study examines the influence of various parameters (such as, thermal storage sizing, commodity prices, time of use tariffs, solar PV integration, etc.) to provide valuable insights into the economic and technical feasibility of energy flexibility in residential buildings under different scenarios. The findings contribute to the development of energy management strategies and flexibility market mechanisms aimed at enhancing grid stability, which is essential to achieve a large penetration share of renewable energy sources into the energy mix.

1. Introduction

Achieving the decarbonisation targets established by the Paris Agreement [1] requires the increase in the share of renewable energy sources (RES). In this context, the European Union (EU) has been a pioneer in RES integration, starting with issuing decarbonisation policies in the mid-nineties [2], and by setting a binding target to cover at least 42.5 % of total energy consumption with renewable sources, with the ambition to reach a 45 % reduction overall by 2030 [3].

Notwithstanding, increasing the penetration of RES leads to significant challenges for conventional power grids, which require a continuous balance between energy demand and generation, usually dominated by a relatively small number of high-output generators [4], to maintain their stability [5]. Due to the intrinsic variability of most renewable

* Corresponding author at: Dipartimento di Ingegneria Meccanica, Energetica, Gestionale e dei Trasporti (DIME). Università degli Studi di Genova, Via All'Opera Pia 15/A, 16145 Genoa, Genoa, Italy.

Email address: mattia.derosa@unige.it (M. De Rosa).

https://doi.org/10.1016/j.apenergy.2025.127038
Received 18 June 2025; Received in revised form 5 September 2025; Accepted 3 November 2025

Available online 11 November 2025
0306-2619/© 2025 The Author(s). Published by Elsevier Ltd. This is an open access article under the CC BY-NC-ND license (http://creativecommons.org/licenses/by-nc-nd/4.0/).

Nomenclature

Abbreviations

AEEF	Available Electric Energy Flexibility
DLMP	Distribution Locational Marginal Price
DR	Demand Response
DSO	Distribution System Operator
EMS	Energy Management Systems
EU	European Union
FT	Flat Tariff
GB	Gas Boiler
HP	Heat Pump
KPI	Key Performance Indicator
MIP	Mixed-Integer Programming
MPC	Model Predictive Control
OC	Operational Cost
PCM	Phase Change Material
PV	Photovoltaic
RES	Renewable Energy Sources
RTP	Real-time Price
SC	Specific (marginal) Cost
SoC	State of Charge
TCL	Thermostatically Controlled Loads
TES	Thermal Energy Storage
TOU	Time-of-use Tariff
TSO	Transmission System Operator
VESS	Virtual Energy Storage System
WT	Weekend Tariff

Symbols

AEEF	Available Electric Energy Flexibility [kWh]
C_{TES}	Thermal capacitance of the TES [kJ/K]
c_p	Heat Capacity [kJ/kgK]
COP	Coefficient of Performance [-]
$COP_{\mathrm{load}}(t)$	COP when the HP is serving the building [-]
$COP_{\mathrm{TES}}(t)$	COP when the HP is charging the TES [-]
G	Total Irradiance [W/m^2]
$GB_{\mathrm{load}}(t)$	GB load when serving the building [kW]
$HP_{\mathrm{load}}(t)$	HP load when serving the building [kW]
$HP_{\mathrm{TES}}(t)$	HP load when serving the TES [kW]
OC	Operational Cost [€]
OC_{DR}	Operational Cost with DR [€]
OC_{noDR}	Operational Cost with noDR [€]
$p_{\mathrm{el}}(t)$	Electricity price [€/kWh]
$p_{el\_threshold}$	Electricity Price Threshold [€/kWh]
$p_{\mathrm{gas}}(t)$	Gas Price [€/kWh]
P_{HP}^{DR}	HP Power Consumption during DR [kW]
P_{HP}^{noDR}	HP Power Consumption during noDR [kW]
P_{DR}	Power consumption during DR [kW]
P_{noDR}	Power consumption during noDR [kW]
SC_{DR}	Specific Cost [€/kWh]
SoC	TES State of charge [-]
T_{mod}	PV module temperature [K]
T_{NOCT}	Nominal Operating Cell Temperature [K]
T_{sink}	Sink Temperature [K]
T_{source}	Source Temperature [K]
T_{TES}	TES Temperature [K]
$T_{\mathrm{TES}}^{\mathrm{max}}$	Maximum TES temperature [K]
$T_{\mathrm{TES}}^{\mathrm{min}}$	Minimum TES temperature [K]
TES_{capacity}	TES Capacity [kWh]
$\dot{Q}_{\mathrm{HP,th}}(t)$	Thermal Power to the TES [kW]
$\dot{Q}_{\mathrm{TES,th}}(t)$	Thermal Power to the building [kW]
$\dot{Q}_{\mathrm{TES,loss}}(t)$	Thermal losses [kW]
U_{TES}	Heat transfer coefficient [W/m^{2}K]
A_{TES}	External Surface Area [m^2]
V	Volume [m^3]
$\Delta T(t)$	Temperature difference [K]
ρ	Density [kg/m^3]

Greek Letters

α	Degradation rate of the PV [-]
α_{DR}	Degree of Power Reduction [-]
β	Tilt angle [rad]
β_{DR}	Demand Response Intensity [-]
γ	Azimuth angle [rad]
δ	Solar declination [rad]
η_{II}	Second-law efficiency [-]
η_{module}	Module Efficiency [-]
η_b	Efficiency of the gas boiler [-]
μ	$p_{\mathrm{el}}(t)$ Average [€/kWh]
σ	$p_{\mathrm{el}}(t)$ Standard Deviation [€/kWh]
θ	Angle of incidence [rad]
Φ	Site latitude [rad]
ω	Hour angle [rad]

resources, such as solar and wind, the deployment of high penetration levels of RES may challenge power system stability [4], potentially leading to disruptions in energy supply.

Over the last decade, demand-side energy flexibility has increasingly attracted significant attention from researchers, companies, and policy-makers as a solution to enhance grid stability and unlock high shares of RES injected into the national power grid. Demand-side flexibility is based on the capability of energy systems to dynamically adapt and optimise their consumption patterns to minimise primary energy consumption and reduce operational costs [6]. For instance, shifting or reducing energy usage during periods of low renewable output or high demand [7,8] leads to a more efficient use of energy resources, while also contributing to a reduction in electricity consumption from the grid.

This paradigm switch from a generation-based flexibility to a distributed-flexibility has led to the concept of flexibility markets – i.e., marketplaces where flexibility services can be traded among users, utilities, producers, and grid operators [5]. These markets incentivise dynamic smart energy management – e.g., by providing financial rewards to those users capable of adapting their energy usage to support grid stability – in order to foster economic opportunities for participants, promote the adoption of advanced technologies and strategies that enable real-time balancing of demand, and increase the potential share of RES [5,8,9].

In this context, the building sector can play an important role in supporting grid stability by providing demand-side flexibility services [10,11], since it represents one of the most energy-intensive sectors [12,13]. A group of buildings may act as a dynamic energy hub, where integrated smart control strategies allow buildings to optimise their consumption patterns to reduce primary energy consumption and operational costs [14]. In addition, they can provide flexibility services to the power grid by participating in Demand Response (DR) programmes [15]. However, the exploitation of building energy flexibility requires a deep understanding of how buildings operate, in order to analyse their energy consumption performance and how they respond to changes in the operational conditions within a short-term horizon.

Generally, unlocking the building energy flexibility requires the deployment of smart energy management systems (EMS) and controllers capable of managing the building energy system (i) to ensure the energy demand is met and (ii) to optimise the energy consumption patterns while exploiting the renewable energy production [16]. Since EMS systems represent a prerequisite to activate flexibility services and to assess their marginal costs, properly designed strategies can significantly minimise costs by synchronising energy consumption with favourable market conditions or renewable energy availability [17], as well as to provide relevant information about the cost associated with potential deviations from optimal control patterns due to the activation of demand-response programs [5,18]. However, many buildings still lack smart energy management systems and sufficient integration with smart grids, limiting their ability to optimise their consumption and to achieve the flexibility readiness required to unlock Demand Response programmes.

Several studies have investigated energy flexibility in buildings, exploring different configurations and control strategies. For instance, [19] investigated the role of advanced control algorithms in optimising energy flexibility and thermal comfort in fully electric buildings. Their findings indicate that shifting electricity consumption from peak to off-peak periods may reduce costs by up to 43 % if intelligent algorithms are deployed. [20] investigated the role of energy flexibility by integrating an indoor phase-change material (PCM) heat exchanger and solar PV with intelligent control. The model consisted of a multi-zone building with roof-integrated PV supplying a heat pump connected to a PCM. Controlled charging/discharging of the PCM aims to stabilize indoor temperatures and reduce heat loss. A MATLAB-based grey-box model simulates the system, and a case study explores optimal design and operation for energy efficiency and flexibility. [21] developed a TRNSYS-based smart integration model that uses predicted energy demand (machine learning, IoT occupancy, weather, load), tariffs, and building performance in a multi-criteria assessment [21]. Results demonstrated about 20 % user bill savings and 25 % retailer cost reduction, with stable environmental impact despite a potential 8 % energy use increase.

Many research studies have shown that the effectiveness of DR depends on the technological setup and control strategies implemented [22]. For instance, the combination of thermostatically controlled loads (TCLs) with predictive control algorithms can significantly enhance the building's flexibility potential [23,24]. [25] analysed a hybrid generator system composed of an air-source heat pump and a gas boiler, integrated with thermal storage, under various DR strategies. Their findings highlighted that the effectiveness of energy flexibility largely depends on the storage capacity and the operational strategy of the system. Furthermore, the study examined the impact of a model predictive control (MPC) strategy on the cost-effectiveness of thermal energy storage (TES). The results showed that TES enables the heat pump (HP) to operate during low-tariff periods, achieving up to 8 % cost savings and reducing CO_2 emissions by up to 13 %. Similarly, [26] examined the interaction between energy markets and building flexibility, focusing on how various market structures impact the flexibility potential of buildings. Their study estimates an average marginal cost of flexibility provision by buildings at approximately 0.03 €/kWh. This relatively low cost highlights the economic viability of leveraging building flexibility as a resource within energy markets. [27] proposed a different approach: a two-stage hierarchical method to optimise the flexibility of Thermostatically Controlled Loads as Virtual Energy Storage Systems (VESS). At the local level, the Distribution System Operator (DSO) schedules TCLs based on the Distribution Locational Marginal Price (DLMP), reflecting the marginal cost of flexibility. At the upper level, the DSO aggregates VESS flexibility and coordinates with the Transmission System Operator (TSO) to provide grid services, enhancing system balance and renewable integration.

Despite these advancements, most studies evaluate energy flexibility at the building level in terms of energy flexibility potential, while the economic aspect is often neglected [25,28]. In particular, standardised methods for assessing both the available flexibility potential and its marginal cost are still an outstanding challenge. The present study therefore takes a step forward in this direction. Generally, the marginal cost represents the cost associated with the shifting or adjusting energy consumption patterns in response to DR signals - e.g., a grid request to reduce (or increase) the consumption at a specific time slot - while still meeting the building operational needs and maintaining the users' comfort [29]. In other words, it quantifies the cost of providing flexibility services for a specific building (or group of buildings), associated with the deviation from the optimal baseline energy consumption pattern [30]. While previous research has demonstrated the benefits of TES and hybrid heating systems, a limited number of studies quantify their impact on operational cost minimisation under different DR strategies and market frameworks [31], especially with renewable-based integrated building energy systems.

In this context, this study investigates the role of buildings in flexibility markets by developing a model for a group of buildings in which energy consumption management is optimised to determine how different energy sources contribute to meeting the load under varying operating conditions. Demand response constraints are introduced to analyse how consumption strategies change when flexibility services are offered to the power system and to quantify the associated economic impact in terms of the marginal cost of flexibility. On this basis, the work proposes an energy flexibility framework that not only evaluates the flexibility potential of a group of buildings but also explicitly incorporates electricity market prices, thereby linking technical operation with economic constraints.

A distinctive contribution is the focus on a cluster of buildings rather than on a single unit, allowing for the assessment of collective optimisation strategies and the synergies enabled by shared flexibility resources and distributed energy systems. This multi-building perspective provides a more realistic and scalable representation of demand-side management, while emphasising the cooperative advantages that enhance economic value.

For this purpose, the aggregation of multiple buildings under a common operator allows flexibility to be pooled and traded more effectively, thereby strengthening the role of buildings as valuable resources for aggregators and as competitive actors in flexibility markets.

The case study consists of a condominium of 4 smart-ready residential buildings equipped with a multi-source hybrid energy system consisting of a heat pump, a gas boiler, photovoltaic panels, and a thermal energy storage. A building energy management system capable of optimising the building consumption pattern based on renewable energy generation and commodities market prices is developed and tested. A notable innovation of this work lies in a deep integration of photovoltaic generation: by synchronising heat-pump operation and storage charging/discharging phases, the controller enhances on-site self-consumption and curtails grid imports. This tight coupling between PV production, thermal storage, and demand-side flexibility distinguishes the framework of this research from existing cost-minimisation studies. The marginal costs associated with the activation of demand-response are then evaluated based on different market scenarios. This approach allows for a more comprehensive evaluation of energy flexibility

Table 1
Summary of building envelope materials and thermal characteristics.

Component	Material/Construction	Thermal Properties
Walls	Exterior cladding (brick) with insulation layer (rigid foam or fiberglass batt)	R-value: R10 (moderate thermal resistance)
Ceilings	Gypsum board and generic interior materials	Thermal conductivity: 0.17 W/m·K (focus on acoustic insulation and fire resistance)
Floors	Insulated carpeted concrete slabs	Thermal mass properties for heat absorption and gradual release
Windows	Simple glazing with low-emissivity coating and possible inert gas fill	U-value: 0.59 W/m^2·K, SHGC: 0.39 (moderate insulation, solar gain control)

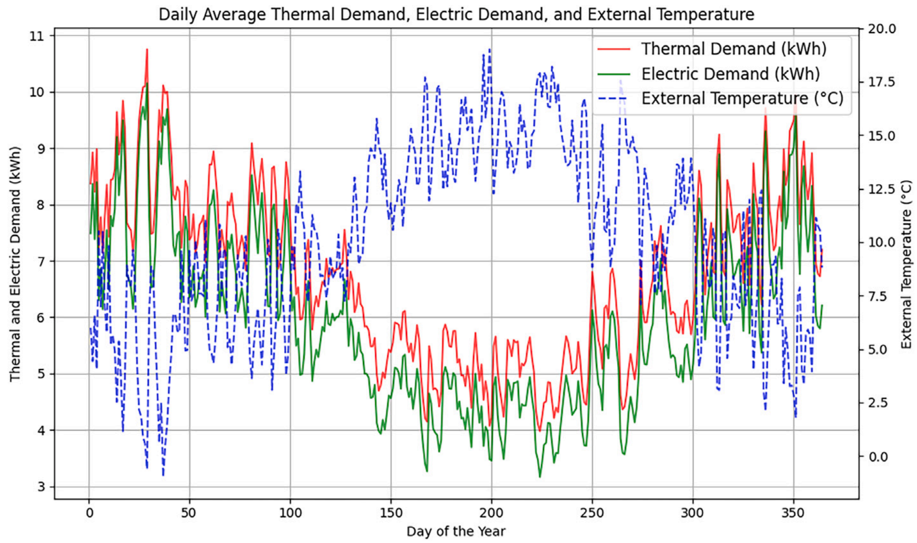

Fig. 1. Energy load of the group of Buildings (thermal and electrical demand) and external temperature over one year.

and its impact on operational cost minimisation. This study also contributes to the literature by evaluating the economic feasibility of TES and hybrid heating systems in a cost-minimisation framework.

The paper is structured as follows: Section 2 details the development of the multi-building energy management system and the optimization framework. Section 3 provides a comprehensive description and analysis of the main results achieved in the study, including the impact of photovoltaic integration and the economic benefits of the TES and hybrid systems under different market scenarios. Finally, Section 4 summarises the key findings and outlines directions for future research.

2. Methodology

2.1. Case study

The case study consists of a condominium of four residential semi-detached houses, with a total gross floor surface of 656 m^2, located in Ireland, which represents a common building archetype frequently found in Irish urban and suburban areas [32]. The buildings are located in a *Cfb* climatic zone[1] according to the Köppen climate classification [33,34].

Being part of the same building complex, the four buildings share the same archetype and, consequently, the same thermophysical characteristics of the building envelope are summarised in Table 1, where details of materials and thermal properties of key construction elements are reported. A calibrated simulation model of the reference archetype, developed in EnergyPlus [35], was used to determine the buildings energy performance and their consumption pattern, which is then aggregated for the subsequent optimisation of the energy system schedule. The simulation was run with a time step of 1 h, which was chosen to balance computational efficiency with the required level of detail for accurately capturing the building's thermal dynamics as suggested by [36,37]. The condominium has a peak thermal consumption of 14.9 kWh and a peak electrical consumption of 11.6 kWh, with a yearly thermal energy consumption of 58.9 MWh and an annual electric energy consumption of 52.1 MWh (corresponding to a group of buildings energy rate of B1, based on the Irish building energy rating classification). The resulting annual profiles in terms of electric and heating energy consumption are shown in Fig. 1, together with the external air temperature. T

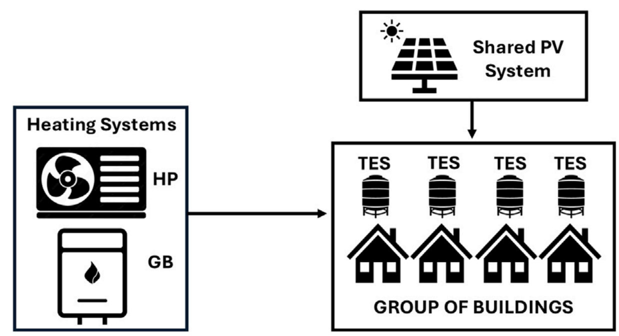

Fig. 2. Energy system scheme.

The four buildings are connected to a shared centralised energy system including a Heat Pump (HP), a Gas Boiler (GB), a Thermal Energy Storage (TES), and a Photovoltaic System (PV), as shown in Fig. 2. The gas boiler serves as a traditional heating source, providing thermal energy when needed, while the heat pump operates in parallel with the boiler. The two technologies are managed to meet the user energy demand, with varying usage percentages to optimise the overall cost and to cover the thermal demand.

The TES consists of a water tank, where excess heat can be stored for subsequent use, and serves the purpose of enhancing the overall energy flexibility of the building energy system. The electricity generated by the shared PV system can be used to power the HP and to cover other building electric loads, contributing to the reduction of the electricity extracted from the national grid.

The following sections describe the numerical models of the building energy systems and related assumptions adopted in the present study. A summary of their principal operational constraints and characteristics is presented in Table 2.

2.1.1. Heat pump model

The HP used in the system is an on-off type, chosen for its simplicity and suitability in applications where continuous modulation of the compressor is not required [38]. The start-up and shut-down of the heat

[1] Cfb: the term C represents a temperate climate where the coldest month average temperature stays between −3 °C and 18 °C; the f denotes fully humid conditions, with consistent rainfall across all months and the b indicates that the warmest month has an average temperature below 22 °C but above 10 °C. Such climatic conditions are typical in Western Europe, including regions like the British Isles.

Table 2
Nominal characteristics and operational constraints of the energy systems.

Component	Key Constraints
Gas Boiler	Efficiency: $\eta_{GB} = 0.96$ Nominal Power: $P_{GB,\max} = 11$ kW
Heat Pump	Type: On-Off Second-Law Efficiency: $\eta_{II} = 0.5$ Nominal Power: 11 kW On/Off Temperature Range: 45 – 55 °C
TES	U-value: $U_{TES} = 0.38$ W/m^2 K Maximum Temperature: $T_{TES}^{max} = 55$ °C Minimum Temperature: $T_{TES}^{min} = 40$ °C TES Capacity: $C_{TES} = 11.6$ kWh/build.
PV system	Installed Peak Power: 11 kWp Module Efficiency: $\eta_{module} = 0.14$ Orientation: 40° tilt, Southeast azimuth Ownership: Shared PV system

pump are governed by the outlet water temperature at the condenser, with an on/off differential controller applying a hysteresis band between 45 °C and 55 °C [39]. The lower threshold triggers the start-up, while the upper threshold forces the shut-down. The on/off heat pump performance is described by the coefficient of performance (COP), expressed with the following equation [26]:

$$\mathrm{COP} = \eta_{II}\left(\frac{T_{sink}}{T_{sink} - T_{source}}\right) \tag{1}$$

where T_{sink} and T_{source} represent the sink and source temperatures respectively, set equal to the external temperature and building heat supply temperature, and η_{II} is the second law efficiency. This approach allows determining the heat pump efficiency under the different working conditions occurring during the year, while reducing the model complexity to ensure fast computation and easing its integration into larger system simulations.

As already mentioned before, the HP can be used to provide the heat demand required by the building or to charge the TES. When the HP directly meets the heating demand, the supply temperature is set equal to the emission system ($T_{emission} = 45\ ^oC$) [40]. On the other hand, when the HP charges the TES, the supply temperature corresponds to the maximum storage temperature ($T^{max}_{TES} = 55\ ^oC$) [41]. In order to compute the COP at each time step, it is necessary to evaluate the term η_{II}, which represents the second-law efficiency of the heat pump. Many scientific articles [42–44] investigate the impact of variability in the second-law efficiency parameter for heat pumps, when different average temperatures between the condenser and evaporator occur. The findings from the literature indicate that this parameter typically remains within a relatively narrow range—i.e., between 0.3 and 0.7—under common operating conditions. Therefore, a constant value of 0.5 has been selected in this study, as suggested by [26].

The sizing of the HP is determined based on [38], who indicates that sizing the unit to satisfy between 59 % to 72 % of the building peak heating load can effectively meet the majority of the annual heating demand, typically around 95 % to 98 %. Based on these considerations, the optimal size of the HP was set at 11 kW of thermal output (with a gross-rated heating COP of 3.7 and a gross-rated cooling[2] COP of 3.1).

2.1.2. Thermal energy storage model

TES systems are typically used to balance supply and demand of heating (and cooling if needed), in order to improve the flexibility of the energy system while optimising resource consumption and operational costs. In case of building applications, water tanks are typically adopted as TES systems due to their low cost and simplicity of installation [26]. In the present study, the TES is modelled as a perfectly mixed water tank [45,46] and is based on the following energy balance equation:

$$C_{TES}\frac{dT_{TES}(t)}{dt} = \dot{Q}_{HP,th}(t) - \dot{Q}_{TES,th}(t) - \dot{Q}_{TES,loss}(t) \tag{2}$$

where T_{TES} and C_{TES} are the temperature and the overall thermal capacitance of the thermal storage. Moreover, the terms $\dot{Q}_{HP,th}(t)$, $\dot{Q}_{TES,th}(t)$, and $\dot{Q}_{TES,loss}(t)$ refer to the thermal power supplied by the HP to the TES, the thermal power delivered from the TES to the building, and the thermal losses from the storage, respectively [47]. The thermal losses from the TES to the external environment are calculated using Eq. (3):

$$\dot{Q}_{TES,loss}(t) = U_{TES}A_{TES}\Delta T(t) \tag{3}$$

where U_{TES} is the typical overall heat transfer coefficient for a water tank, which is assumed equal to 0.35 W/m^{2}K [48,49], A_{TES} is the external surface area, while $\Delta T(t)$ is the temperature difference between the storage temperature and the surrounding environment [25]. Based on the TES temperature obtained by Eq. (2) at each time step, it is possible to define its state of charge (SoC), which indicates the current level of stored energy relative to the system's total capacity, as shown in the equation below:.

$$\mathrm{SoC} = \frac{T_{TES} - T_{TES}^{min}}{T_{TES}^{max} - T_{TES}^{min}} \tag{4}$$

where $T_{TES}^{max} = 55\,°C$ [41,50,51] is the maximum storage temperature when the heat pump serves the TES, and $T_{TES}^{min} = 40\,°C$ [41] is the minimum storage temperature allowed.

This expression accounts for the range of operating temperatures of the TES, allowing for the assessment of the stored energy relative to its capacity, which can be calculated based on the following expression:

$$\text{TES capacity} = C_{TES}\Delta T_{TES}\left(\frac{1}{3.6\times10^3}\right) \tag{5}$$

where $\Delta T_{TES} = 20$ K [52] is the temperature difference considered in the storage.

The thermal capacitance of the thermal energy storage system, C_{TES}, is calculated using the following equation [45,46,53]:

$$C_{TES} = \rho \cdot V \cdot c_p \tag{6}$$

where ρ is the heat transfer fluid's density, V is the tank's volume, and c_p is the fluid's specific heat capacity. Considering the physical properties of water and a volume of 0.5 m^3, the thermal capacitance for each building is 2093.5 kJ/K.

This leads to a TES capacity of 11.6 kWh per household, which is appropriate for residential applications because it aligns with typical daily heating and hot water demands. Such capacity enables effective storage of surplus thermal energy generated by the heat pump, particularly during periods of low electricity prices or high renewable energy availability. In the present case study, each building is equipped with its own 0.5 m^3 TES unit. This setup allows flexibility to be assessed at the building level and aggregated at the condominium scale.

2.1.3. Photovoltaic panels model

To serve the entire building complex, a shared PV system [54] with a total installed peak capacity of 11 kWp is used. The power generated by this central system is equally distributed among the four buildings.

The efficiency of the PV system (η_{module}) is 0.14 and a fixed open rack configuration is adopted. This configuration keeps the panels at a constant angle and orientation, while the open rack design allows for proper ventilation, preventing overheating and maintaining panel efficiency.

[2] Due to Ireland's temperate climate, the cooling load for a typical building is often considered negligible or non-existent.

The numerical model adopted in this study calculates the real-time power output of the PV system based on the solar irradiance, PV module efficiency, and the panel capture area based on the incident solar radiation [55]. Generally, the total irradiance on the tilted surface is given by the following equation [56]:

$$G = I_{bd}\cos\theta + I_{d0}\frac{1+\cos\beta}{2} \tag{7}$$

where θ represents the angle of incidence, and it depends on solar declination (δ), hour angle (ω), site latitude (Φ), panel tilt angle (β), and panel azimuth angle (γ). It is estimated as [56]:

$$\begin{aligned}\cos\theta &= \sin\delta\,(\sin\Phi\cos\beta - \cos\Phi\cos\beta\cos\gamma)\\ &\quad + \cos\delta\,(\cos\Phi\cos\beta - \sin\Phi\cos\beta\cos\gamma)\cos\omega\\ &\quad + \cos\delta\sin\beta\sin\gamma\sin\omega \end{aligned} \tag{8}$$

PV panels are oriented with a tilt angle of 40° and with a SE azimuth orientation to position them for effective sunlight capture based on the site's specific geographical conditions [57]. The module efficiency is influenced by the temperature and is computed using the relation [58,59]:

$$\eta_{\text{module}} = \eta_{T_{\text{ref}}}\left[1 - \alpha(T_{\text{mod}} - T_{\text{NOCT}})\right] \tag{9}$$

where:

- α is the degradation rate of the PV
- T_{mod} is the PV module temperature
- T_{NOCT} is the Nominal Operating Cell Temperature

To compute the energy generated by the PV system it is important to account for inverter and cable losses, as they reduce the usable energy and ensure a realistic assessment of system performance.

2.2. Demand-side management

Demand-side management is characterised by the optimisation of energy consumption patterns and by the balance between demand and supply through various strategies. Its effectiveness is influenced by the system costs, tariff structures, and control methodologies, which determine its overall impact on energy efficiency and grid stability, as outlined in the following sections.

2.2.1. Operational cost of the system

The operational cost (OC) of the energy system is described by a cost function that accounts for both the electricity cost associated with the heat pump operation and the gas cost for running the gas boiler. The mathematical expression for the operational cost can be written as follows [26]:

$$OC = \sum_{t\in T}\left[\left(\frac{HP_{load}(t)}{COP_{load}(t)} + \frac{HP_{TES}(t)}{COP_{TES}(t)}\right)\cdot p_{el}(t) + \frac{GB_{load}(t)}{\eta_b}\cdot p_{gas}(t)\right] \tag{10}$$

where:

- $t \in T$: Each time period in the simulation or operation over the time horizon T.
- $HP_{\text{load}}(t)$: heat pump thermal output needed to meet the building's heating demand.
- $COP_{\text{load}}(t)$: coefficient of performance of the HP at time t.
- $HP_{\text{TES}}(t)$: heat pump thermal output needed to charge the TES at time t.
- $COP_{\text{TES}}(t)$ coefficient of performance of the HP while charging the TES at time t.
- $p_{\text{el}}(t)$: Electricity price at time t.
- $GB_{\text{load}}(t)$: thermal output of the gas boiler to meet the heating demand at time t.
- η_b: Efficiency of the gas boiler.
- $p_{\text{gas}}(t)$: Real-time gas price at time t.

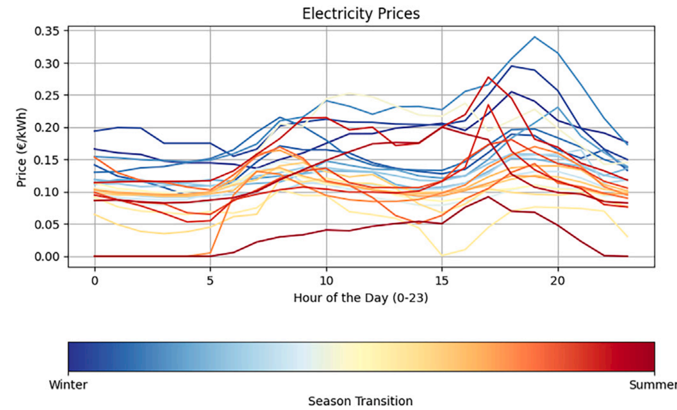

Fig. 3. Daily Real Time Price for one year.

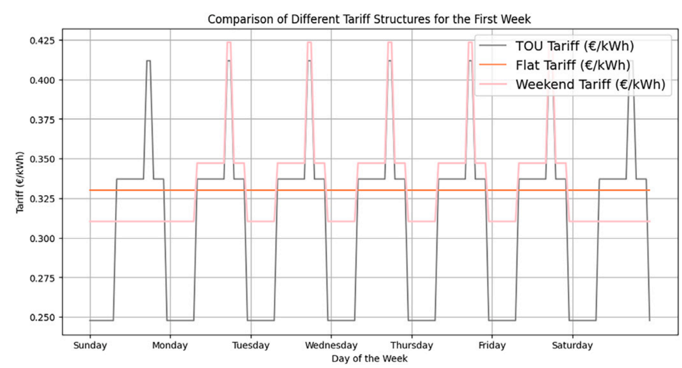

Fig. 4. Flat, Time of Use and Weekend electricity prices.

2.2.2. Electricity and gas tariffs

In the present work, a smart controller is implemented to optimise the energy system operation by minimising operational costs (i.e., objective function) in response to price signals to look for a rational and cost-effective energy use while ensuring that the building energy demands are met. Tariffs directly influence the controller decisions and the optimisation process, determining how the demand is met by the energy system to minimise costs. For this reason, various electricity tariff options – such as real-time pricing (RTP), flat tariffs (FT), time-of-use tariffs (TOU), and weekend tariffs (WT) – have been considered to better manage energy generation and improve cost efficiency.

RTP is a dynamic electricity pricing model where the cost of electricity fluctuates based on real-time market conditions [60].

Typically, high RTP prices indicate periods with high energy demand, which also correspond to the most expensive power plants being dispatched to meet consumption needs. The colour gradient in Fig. 3 provides insight into seasonal trends in electricity pricing (blue tones indicate the winter season, while red tones indicate the summer; lighter shades represent the transition seasons, i.e., spring and autumn.

The other types of tariffs, illustrated in Fig. 4, were obtained by considering actual electricity tariffs typically used in Ireland [61]. The flat tariff maintains a consistent rate throughout the day, providing simplicity in billing. On the other hand, the TOU tariff shows a variation in the electricity price based on the time of day, with higher rates occurring during peak periods (e.g., 5 pm to 7 pm for electricity) to encourage consumers to shift their usage to off-peak hours (e.g., night or early morning). Finally, the weekend tariff offers different rates for weekends compared to weekdays. In particular, during the weekends the tariff is flat while during the weekdays the tariff has a shape similar to the TOU tariff [61].

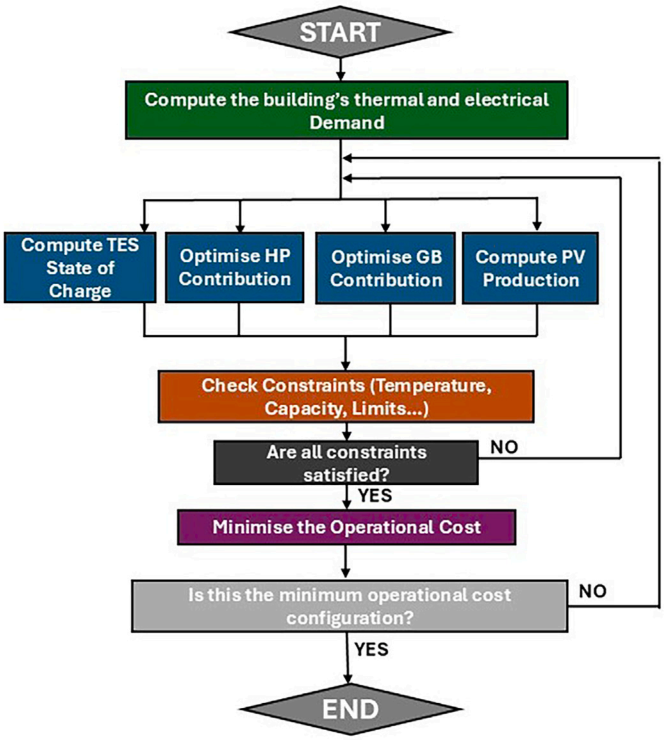

Fig. 5. Flowchart of the energy management optimization process for integrated building systems.

Finally, the gas price is derived from data provided by the Eurostat Database[3] [62].

2.2.3. Optimisation algorithm

The Optimisation algorithm adopted in the present study is a Mixed-Integer Programming (MIP), solved using the GNU Linear Programming Kit (GLPK). The problem is formulated as a set of linear (and non-linear) equations and inequalities, with some variables restricted to integer values [63]. The objective is to find the optimal solution that satisfies all the constraints while minimising (or maximising) a specific objective function. MIP is widely used in fields such as operations research, logistics, and energy management due to its ability to handle discrete decision variables, making it suitable for problems that involve on/off decisions, scheduling, and resource allocation [64,65]. In the MIP formulation, the problem is structured around a set of decision variables and parameters. The decision variables represent the values that the optimisation algorithm will determine to minimise the cost or meet other objectives, while the parameters are known values that characterise the system's constraints and behaviour.

Fig. 5 shows the key constraints and the primary behaviour of the optimisation algorithm. This algorithm is designed to solve an optimization problem where the main goal is to reduce operational costs. The objective function of the optimisation problem used in this study is the minimisation of the operational costs (OC), as shown in the equation below:

$$\min \left\{ \sum_{t \in T} \left[\left(\frac{HP_{load}(t)}{COP_{load}(t)} + \frac{HP_{TES}(t)}{COP_{TES}(t)} \right) \cdot p_{el}(t) + \frac{GB_{load}(t)}{\eta_b} \cdot p_{gas}(t) \right] \right\} \tag{11}$$

[3] In the first semester of 2023, the gas price for household consumers was 0.147 €/kWh, increasing to 0.165 €/kWh in the second semester.

The constraints are designed to ensure both thermal and electrical balance within the system. Formally, the thermal and electrical balances can be expressed as follows:

$$Q_{demand}(t) = Q_{HP}(t) + Q_{GB}(t) + Q_{TES,dis}(t) \tag{12}$$

$$E_{demand}(t) = E_{PV}(t) + E_{grid}(t) \tag{13}$$

where $Q_{demand}(t)$ is the thermal demand at time t, $Q_{HP}(t)$ and $Q_{GB}(t)$ are the thermal contributions of the heat pump and the gas boiler, respectively, while $Q_{TES,dis}(t)$ represents the TES discharging. $E_{demand}(t)$ is the electrical demand, covered by the photovoltaic production $E_{PV}(t)$ and by the electricity purchased from the grid $E_{grid}(t)$.

For the TES charging process, a key constraint states that the energy stored equals the heat pump's output allocated for storage along with any excess electricity generated by the PV system.

Another important constraint governs the operation of the TES, specifically managing its temperature dynamics at each time step to maintain proper thermal regulation (within the thermostatic set-points). Regarding the heat pump operation, specific constraints ensure that its output, used to meet building energy demands and charge the TES, aligns with its operational status, preventing energy delivery beyond its capacity. Additionally, the energy supplied by the PV system to cover the building's energy demand is constrained to not exceed its actual production. The TES charging and discharging processes are also regulated to prevent overcharging or excessive discharging, depending on its current operation mode. An additional constraint enforces that the TES temperature remains within predefined safety and efficiency limits, preserving system stability and optimal performance. Finally, the constraints ensure that the heat pump is always active during TES charging, establishing a direct link between the two processes. A detailed mathematical formulation of each component is provided in Section 2.1. In that section, all governing equations are presented to describe their operational behaviour and dynamic interactions within the optimisation framework.

2.3. Demand response framework

Demand Response (DR) is a strategy aimed at adjusting the energy consumption of end-users in response to market signals or grid stability requirements. The primary goal is to enhance grid reliability, prevent overloads, and reduce energy costs by shifting or reducing consumption during peak demand periods [66]. DR aims to adjust the power usage of certain devices, such as heat pumps, in response to fluctuating electricity prices or grid conditions.

The type of DR used in the present work involves a price-based approach that calculates a threshold for the electricity price. Typically, high market prices indicate periods of high demand for electricity, during which a load reduction may be enforced to reduce the stress on the grid [67]. In this context, price-based demand response becomes particularly effective as it aligns user consumption with the grid's operational needs. For instance, the price-based approach is commonly used in the literature [25,26,51,67,68] since it provides an effective method for demand response based on market signals and grid conditions.

In the present study, when the market price exceeds the threshold, DR is triggered to reduce the HP power consumption. This threshold is computed by considering the daily average electricity price (μ_{el}) and the standard deviation of the electricity price (σ_{el}), as shown in Eq. (14). The term β_{DR} is the DR intensity and is added to increase/decrease the threshold value for sensitivity analysis.

$$p_{el\_threshold} = \mu_{el} + \beta_{DR} \cdot \sigma_{el} \tag{14}$$

This approach ensures that DR is triggered during periods of high electricity prices: when the electricity price exceeds $p_{el\_threshold}$, DR is activated, and the power consumption of the HP, represented by P_{HP}^{DR}, is adjusted according to the DR intensity factor, α_{DR}. The heat pump power consumption in case of DR activation is calculated with the following equation:

$$P_{HP}^{DR} = P_{HP}^{noDR} - P_{HP}^{noDR} \cdot (1 - \alpha_{DR}) \quad (15)$$

where P_{HP}^{ref} is the reference power consumption of the HP without demand response. The DR intensity, α_{DR}, is a parameter that ranges from 0 to 1 and controls the degree of power reduction:

- $\alpha_{DR} = 0$: This corresponds to no demand response (0 % DR), meaning that the heat pump operates at its nominal power, P_{HP}^{noDR}.
- $\alpha_{DR} = 1$: This represents full demand response (100 % DR), when the heat pump is shut down and the DR power reduction is maximized.
- $0 < \alpha_{DR} < 1$: Indicates partial demand response, with the power consumption reduced in proportion to the value of α_{DR}, providing a flexible adjustment to different levels of grid demand or price signals.

The assessment of DR programs in buildings is challenging due to the lack of standardised metrics for evaluating energy flexibility. To address this, specific key performance indicators (KPIs) are introduced to provide a consistent framework for evaluating the flexibility potential from technical, economic, and energy perspectives [24,26,69]. In particular, this study adopts two main relevant KPIs, namely the Available Electric Energy Flexibility (AEEF) and Specific Marginal Costs (SC). The AEEF measures the variation in the building electrical energy consumption due to the activation of DR programs over a specific period, and it is calculated as shown in the equation below:

$$\text{AEEF}(t) = \int_0^t |P_{\text{DR}} - P_{\text{noDR}}| \, \mathrm{d}t \quad (16)$$

where P_{DR} is the power consumption during DR actions, P_{noDR} is the power consumption during no Demand Response operation, and t represents the time period over which DR is evaluated.

The SC represents the specific cost associated with a particular DR program, calculated by the ratio between the net DR operational costs and the available energy flexibility:

$$\text{SC}_{\text{DR}} = \frac{(OC_{\text{DR}} - OC_{\text{noDR}})}{\text{AEEF}_t} \quad (17)$$

where OC_{DR} and OC_{noDR} are the operational costs with and without DR events respectively, while AEEF_t is the Available Electric Energy Flexibility over time t. These KPIs are used to quantify the impact of DR actions in terms of reduction of energy consumption and the associated (marginal) costs, which represent fundamental information for aggregating DR profiles among different buildings and unlocking the participation of networks of buildings in energy flexibility markets.

3. Results and discussion

The methodology described in the previous section was employed to analyse the capability of the reference building blocks to exploit the energy flexibility provided by the integrated energy system. To provide a detailed analysis of the results, the findings are structured into different sections, each focusing on a key aspect of the system's performance. First, the impact of different electricity market prices is analysed (Section 3.2). Second, a demand response analysis examines how the buildings dynamically adjust their aggregated consumption (Section 3.3). Afterward (Section 3.4) the role of the TES is evaluated and (Section 3.5) the impact of the PV panels is analysed. Finally, a general analysis of all scenarios is presented (Section 3.6).

Each simulation was carried out over a representative winter week, selected to capture the typical boundary conditions and thermal loads of the heating season. A temporal resolution of one hour was adopted, as this time step provides a good balance between computational efficiency and the ability to reproduce the dynamic behaviour of the system.

3.1. Scenarios and baseline definition

In order to assess the performance of the building complex, four reference scenarios were defined. The scenarios are primarily differentiated by the electricity tariff schemes, which play a key role in this analysis since the study specifically addresses the interaction with flexibility markets and the resulting costs of flexibility.

Scenario A considers a real-time pricing scheme that reflects actual variations in electricity market conditions, while, Scenario B applies a time-of-use structure with differentiated day and night prices. Then, Scenario C represents the weekend tariff, and Scenario D considers the flat tariff. In all four cases, the reference baseline corresponds to conventional operation without demand response (No-DR), and the TES capacity was fixed at 0.5 m^3. In contrast, the DR case considers a demand response intensity parameter β_{DR} equal to 1, while maintaining the same TES capacity of 0.5 m^3. Subsequently, starting from the results obtained in Section 3.2, a sensitivity analysis was carried out starting from Scenario A. The following parameters were varied: the demand response intensity, the thermal energy storage size, and the natural gas price, in order to assess their impact on both system available flexibility and the overall flexibility marginal cost.

3.2. Influence of electricity market prices

The influence of different electricity tariff structures (RTP, TOU, WT, and FT) and their impact on the weekly operational cost both without and with DR, as well as on the flexibility KPIs is analysed in Table 4. The analysis is conducted over one representative winter week. The RTP tariff is the most favourable tariff structure from a flexibility point of view, showing the highest AEEF value, which indicates a greater flexibility potential (i.e., the system better adapts to external signals and renewable energy availability). Furthermore, the operational costs under RTP structure turn out to be the lowest among the tariffs, since the use of RTP allows for a more rational and cost-optimised energy supply.

The TOU and Weekend tariffs show higher operational costs compared to the RTP scenario, with an increase in case of DR activation, and lower AEEF values (84.06 and 72.44 kWh, respectively). This indicates that the DR under these tariffs provides more limited space for the exploitation of the energy flexibility, as the price signals are more predictable and less dynamic.

Observing the results in terms of marginal costs of the energy flexibility harnessed under the three tariff scenarios, it is evident that the Weekend tariff shows the lowest values (0.0735 €/kWh), making it the most cost-effective scheme for leveraging demand flexibility. This is because the Weekend tariff applies a constant price, equal to the night-time rate, which is the lowest in the tariff structure [61]. As a result, shifting energy consumption to the weekend period incurs minimal additional

Table 3
Definition of the reference scenarios.

Scenario	Tariff	Baseline scenario	DR scenario	TES size [m^3]
A	Real-Time Price	No-DR	$\beta_{\text{DR}} = 1$	0.5
B	Time-of-Use	No-DR	$\beta_{\text{DR}} = 1$	0.5
C	Weekend	No-DR	$\beta_{\text{DR}} = 1$	0.5
D	Flat	No-DR	$\beta_{\text{DR}} = 1$	0.5

Table 4
Comparison between different tariff structures of OC without and with DR, AEEF and SC over one winter week.

Tariff Structure	OC no DR	OC DR	AEEF	SC
Unit	[€]	[€]	[kWh]	[c€/kWh]
RTP (Scenario A)	57.05	70.13	119.82	10.90
ToU (Scenario B)	93.06	100.08	84.06	8.35
Weekend (Scenario C)	98.83	104.16	72.44	7.36
Flat (Scenario D)	97.53	97.53	0	0

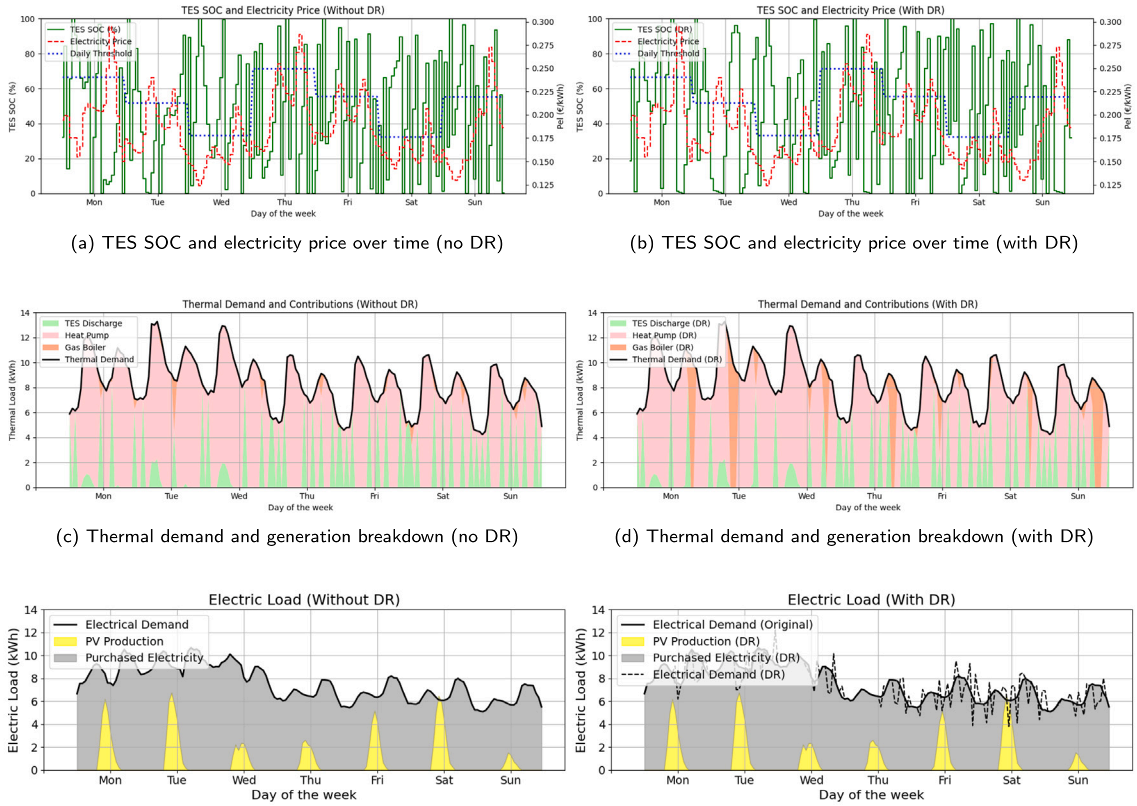

(a) TES SOC and electricity price over time (no DR)

(b) TES SOC and electricity price over time (with DR)

(c) Thermal demand and generation breakdown (no DR)

(d) Thermal demand and generation breakdown (with DR)

(e) Electric load and PV production (no DR)

(f) Electric load and PV production (with DR)

Fig. 6. Comparison of system behaviour with and without Demand Response strategies over one winter week (Scenario A).

costs, maximising the use of demand flexibility. However, while the Weekend tariff offers the lowest marginal cost, the RTP tariff provides a greater flexibility potential by adapting to real-time price signals, even though its marginal cost is higher (0.1232 €/kWh). Based on these observations, the RTP tariff (Scenario A) is selected for deeper investigation in the following part of this section, as it is associated with the lowest operational costs (OCs) and allows for harnessing a greater amount of energy flexibility potential, offering valuable insights into more dynamic and responsive energy management. All subsequent sensitivity analyses are therefore carried out with reference to Scenario A (RTP).

3.3. Operating conditions and demand response (DR) assessment

Fig. 6 illustrates the system operation with and without the activation of the demand response measures. Generally, the DR strategy influences the TES by modifying the charging and discharging patterns based on electricity price variations. This is highlighted in Fig. 6(a), (b) which show the hourly electricity price trend, together with the daily threshold (Section 2.3), and the SoC of the TES. Moreover, it can be noted that the SoC increases before the electricity price exceeds the threshold and then decreases during the hours in which the DR is active.

Observing the building thermal load pattern and the share of each energy system that contributes to meeting the demand (Fig. 6(c), (d)) it can be noted that, while the thermal demand is the same in both cases, the activation of DR measures constrains the HP operation to avoid operating when the electricity price exceeds the daily threshold. This restriction forces the system to rely more on TES discharge and on the gas boiler to meet thermal energy demand.

This is confirmed in Fig. 6(e), (f) which shows the total electrical load of the building, including a base load—mainly from household electrical appliances—and a variable component resulting from the electricity consumption of the heat pump. The difference between the framework with and without DR highlights how DR reduces the heat pump operation during expensive hours and increases it during cheap hours, effectively reshaping the building electricity consumption profile. Additionally, the electric consumption profiles show a typical rebound effect consisting of an increase in electricity consumption before or after the DR period—due to thermal energy storage charging—and a subsequent decrease during the TES discharging phase. This response is driven by the optimisation algorithm, which proactively anticipates the DR event and strategically adjusts the system operation to reduce costs while meeting the thermal energy demand.

The analysis is further detailed in Fig. 7, which outlines the difference in HP consumption patterns between the DR and no-DR cases. In this figure, bars indicate when the HP operates more (red) or less (green) for the DR case compared to the no-DR case. It is evident that under DR, the HP reduces its operation during periods of high electricity prices, while it increases usage in more cost-effective hours. This confirms that optimisation algorithms are capable of shifting the building energy consumption in a DR response framework.

Additionally, Fig. 8 illustrates the variation over time of the TES state of charge (SoC) in both cases with and without DR. The red and blue lines represent the TES SoC in the no-DR and DR cases, respectively, while grey areas indicate high electricity price periods. The results show that TES can effectively contribute to augmenting the energy flexibility potential of the building energy system, since it allows the load shifting during high-price periods, especially in a DR scenario when the HP is forced to reduce its load as the DR action is triggered.

As explained in Section 2.3, the DR action is induced by the price threshold, and its influence on the energy flexibility potential is investigated. A specific criterion was selected based on electricity price signals (Eq. (14)) determined by the daily average electricity price, the standard deviation and the DR intensity β_{DR}. Setting $\beta_{DR} = 0$ implies that the threshold corresponds to the mean daily price, leading to a much more frequent and prolonged activation of the DR signal compared to

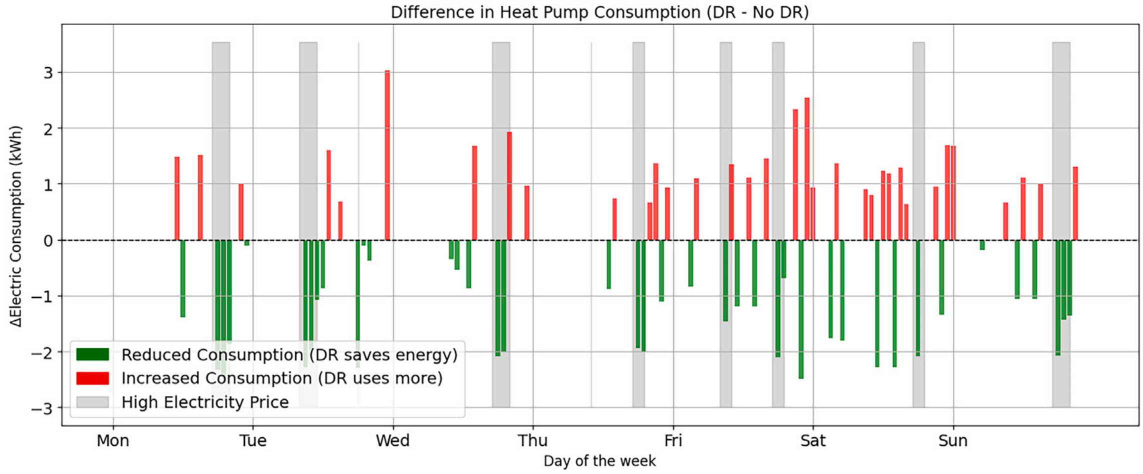

Fig. 7. Difference in heat pump consumption between no-DR and DR scenarios (Scenario A).

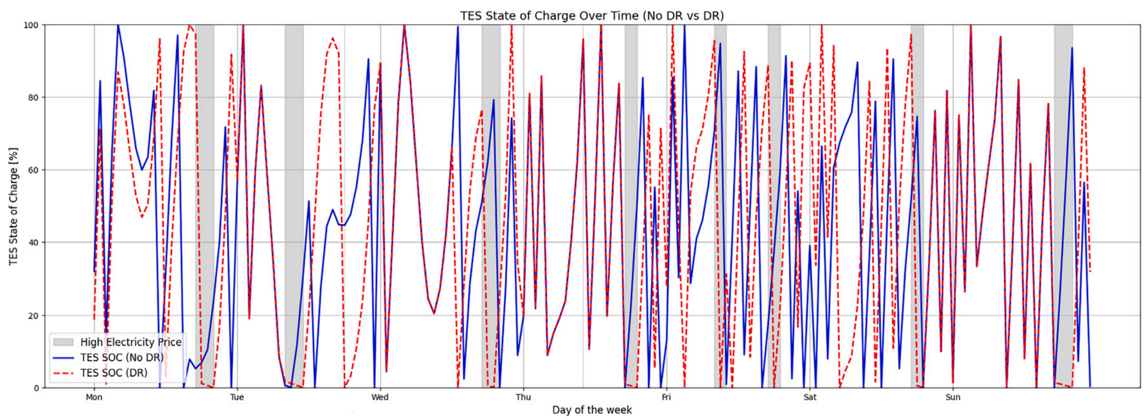

Fig. 8. TES discharge timing comparison between no-DR and DR cases (Scenario A).

the baseline case described in Section 3.6, where β_{DR} was set to 1. As a result, the system experiences significantly different operational dynamics, with flexibility being exploited more extensively throughout the day (Fig. 9). However, the trade-off is that the system experiences more frequent state changes, which could increase operational complexity and uncertainty.

Table 5 compares the results obtained by selecting different values of the DR intensity β_{DR} (Eq. (14)). It can be observed that the operational costs in the configuration without DR remain constant. When compared to the reference case with $\beta_{\mathrm{DR}} = 1$, the costs decrease for $\beta_{\mathrm{DR}} = 2$, whereas they increase significantly for $\beta_{\mathrm{DR}} = 0$. The Available Electric Energy Flexibility (AEEF) shows a similar trend, being lower with $\beta_{\mathrm{DR}} = 2$ while reaching higher values with $\beta_{\mathrm{DR}} = 0$. With $\beta_{\mathrm{DR}} = 2$, the threshold for activating the Demand Response (DR) service is higher, leading to shorter DR operation. This selective activation allows the building to remain closer to its optimal operating point, minimising unnecessary load shifting and reducing the impact of the DR actions on the overall operating costs. Since the system only responds during periods of significant price peaks, it avoids minor adjustments that bring limited energy shifting. Furthermore, the cost of flexibility is the lowest for $\beta_{DR}=2$ (0.0291 €/kWh), indicating a lower marginal cost of the flexibility available, despite the lower AEEF. In contrast, with $\beta_{DR}=0$, the system reacts more frequently to price fluctuations, resulting in more frequent load shifts that are not always economically justified. This excessive sensitivity increases the marginal cost of flexibility dramatically, reaching 0.2469 €/kWh, reflecting economic inefficiencies and higher operational expenses.

This analysis highlights the importance of fine-tuning the DR threshold to achieve an optimal trade-off between energy savings, cost-effectiveness, and operational feasibility. It is also important to observe that DR can be triggered not only by market price signals, but by grid-related needs, such as frequency deviations (for primary, secondary, or tertiary regulation), voltage fluctuations, or power imbalances. In these cases, the activation of DR responds directly to the operational requirements of the grid rather than to economically-driven criteria [70].

3.4. The role of thermal energy storage

The optimal sizing of thermal energy storage systems is a critical design parameter that directly influences both operational performance and economic viability. TES serves as a key enabler for efficient energy management, particularly in frameworks involving the integration of variable renewable energy sources, Demand-side management, and Demand Response. Therefore, the impact of TES sizing on the energy flexibility potential (AEEF) and its specific cost (SC) has been evaluated with the aim of assessing how variations in TES capacity affect the system capability to provide energy flexibility services.

Figs. 10 and 11 illustrate the SC and the AEEF as functions of the TES volume per building, with daily values plotted alongside the variability observed. On the technical side, increasing the TES volume enhances the energy storage capability, impacting the overall system flexibility potential and its capability to meet fluctuating thermal demands. However, larger volumes also lead to higher thermal losses and potential inefficiencies if the stored energy is not optimally utilised [71].

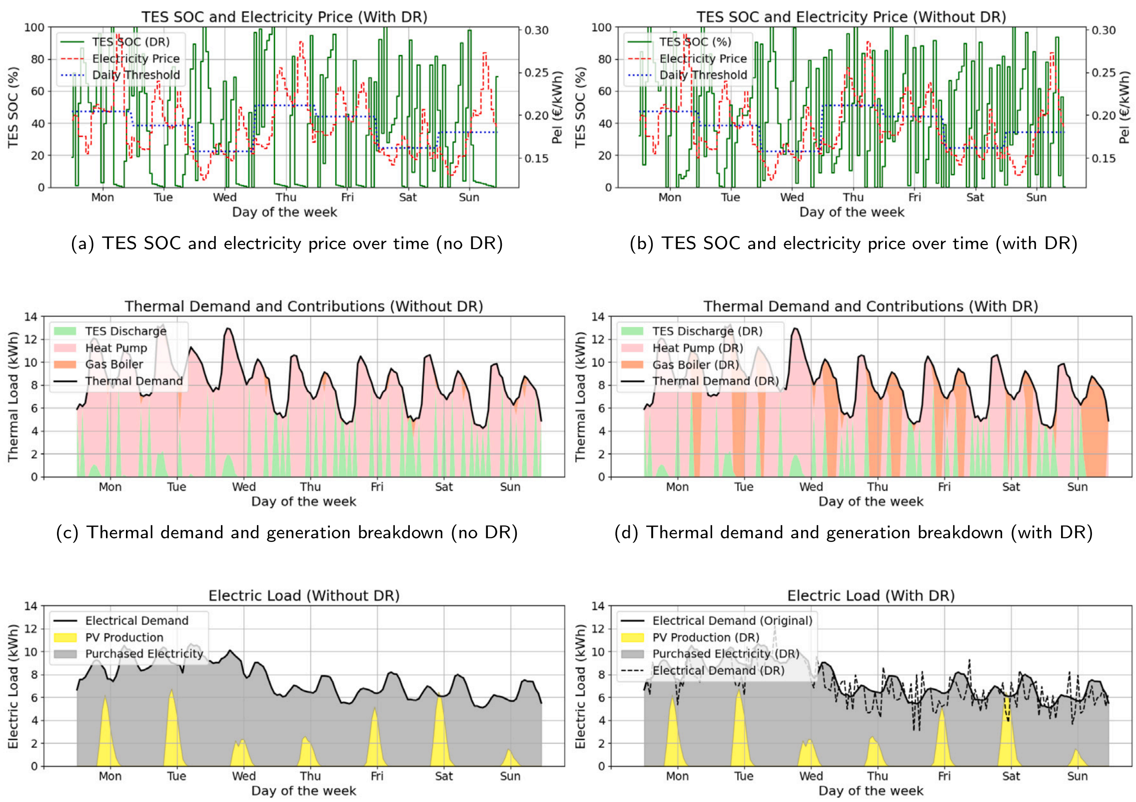

(a) TES SOC and electricity price over time (no DR)

(b) TES SOC and electricity price over time (with DR)

(c) Thermal demand and generation breakdown (no DR)

(d) Thermal demand and generation breakdown (with DR)

(e) Electric load and PV production (no DR)

(f) Electric load and PV production (with DR)

Fig. 9. Comparison of system behavior with and without Demand Response strategies over one winter week ($\beta_{DR} = 0$).

Table 5
Comparison of the operational costs and the flexibility KPIs for different DR situations over one winter week.

DR Intensity	OC no DR	OC DR	AEEF	SC
	[€]	[€]	[kWh]	[€/kWh]
$\beta_{DR} = 0$	57.05	97.26	216.06	0.2469
$\beta_{DR} = 1$	57.05	70.13	119.82	0.1232
$\beta_{DR} = 2$	57.05	59.34	78.42	0.0291

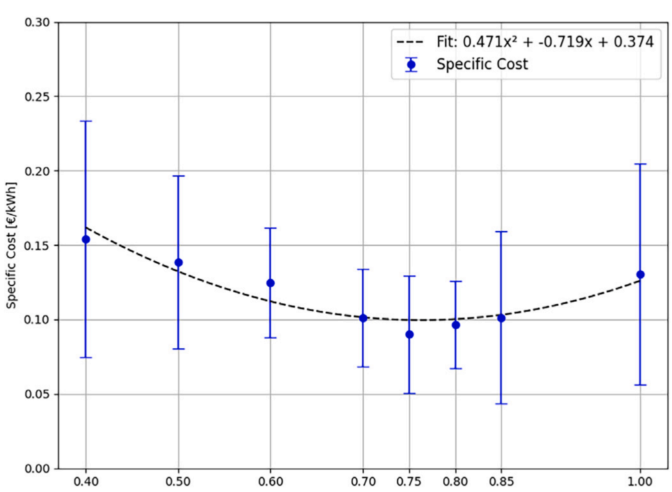

Fig. 10. Specific Marginal Cost as function of the TES volume per building.

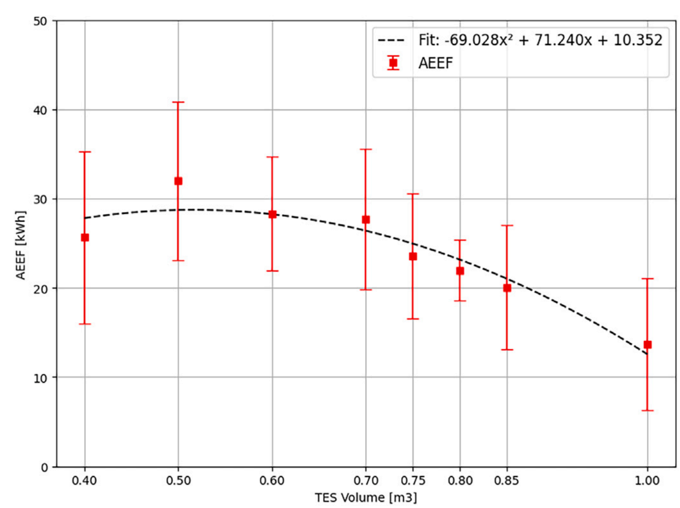

Fig. 11. Available Electric Energy Flexibility as function of the TES volume per building.

To better understand the relationship between flexibility KPIs and the TES volume, trend curves were fitted to the data obtained from the analyses. Starting from Fig. 10, it is possible to observe that the flexibility cost initially decreases as the TES volume increases, reaching a minimum value at approximately 0.75 m^3 per building. Higher values of TES thermal capacity do not offer any significant reduction in energy costs

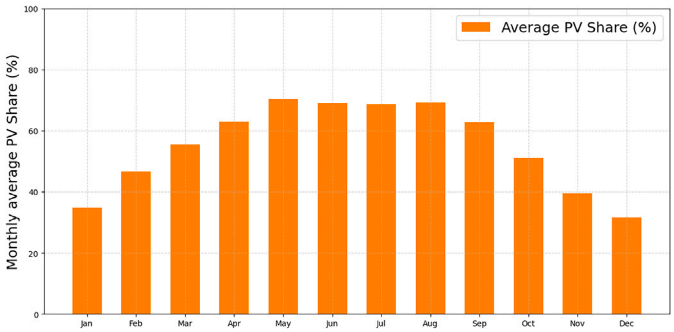

Fig. 12. Building Electrical Load.

or any load-shifting improvements. In these conditions, the TES can be considered oversized compared to the energy flexibility needed, which causes inefficiencies from an operational point of view. This is also confirmed by Fig. 11, which shows a non-linear trend of the AEEF versus the TES volume, with a maximum value for lower capacity (about 0.5 m^3 TES per building). Therefore, it is possible to conclude that the choice of 0.5 m^3 per building aligns with the observed trends, since it ensures a reasonable trade-off between SC, AEEF, and practical implementation constraints.

3.5. The role of the photovoltaic panels

The integration of PV panels allows to directly offsetting part of the building electrical demand, flattening peaks and lowering grid reliance [52].

Fig. 12 highlights the annual impact of PV generation on the building electricity consumption, in terms of average monthly share of demand covered by the solar production. During the winter season, the PV system covers roughly 30–35 % of the building load, and reaches a maximum value of about 70 % during the summer season.

The Net Load represents the building total electrical demand after accounting for the energy generated by photovoltaic panels. It is calculated as the difference between the building original consumption and the electricity produced by the PV system. This metric allows one to understand how much energy still needs to be supplied by the grid, particularly during periods of high demand.

Fig. 13 depicts the building's electrical demand, comparing scenarios with and without rooftop PV, as well as with and without demand response (DR). As expected, the deployment of a PV system reduces the electric energy extracted from the grid. When DR is introduced, the demand curve is further levelled by shifting flexible loads into lower-price periods, yielding a smoother and consistently reduced load profile throughout the afternoon and evening. Over the course of each day, PV generation drives a pronounced midday reduction in net demand, reducing peak loads by roughly 40–50 % compared to the baseline, and in some instances pushing net consumption to near zero or slight export around solar noon. When DR is activated on top of PV, flexible loads are shifted into these high-generation time-slots, resulting in an additional 10–15 % reduction of the remaining peaks and a noticeably smoother demand curve throughout the afternoon and early evening.

3.6. Discussion

This section discusses a comparative analysis of the different scenarios considered, which explores the influence of several parameters – commodity prices, electricity tariff structures, and thermal storage volumes, while also considering the influence of different levels of Demand Response strategies – to assess their combined effects on the building's energy flexibility KPIs.

Fig. 14 illustrates the weekly operational costs over a representative winter week. The results are presented both without and with demand response, including the three reference electricity tariff scenarios (RTP, ToU, and Weekend). The flat tariff is not considered, as it cannot provide flexibility under the adopted criterion, which relies on threshold values and price signals. In addition, starting from the RTP reference case (Scenario A), the figure also reports the outcomes of the sensitivity analysis, in which the thermal energy storage size, the demand response intensity (β_{DR}), and the natural gas price were varied separately. Activating the DR leads to an increase in operational costs across all cases, which can reach a 70 % increment. For instance, adopting a low activation threshold ($\beta_{DR} = 0$ scenario), the operational cost increases by 70 %, making it the most expensive configuration from a DR perspective. Similarly, other cases – such as the scenario with a 20 % increase in the gas price and the scenario that uses the Time of Use Tariff – also result in a significant increment in operational cost, i.e., 29 % and 23 %, respectively. Conversely, the scenario with $\beta_{DR} = 2$ presents the lowest increase (4 %), suggesting that fewer DR hours lead to lower operational costs (but with low available energy flexibility potential).

Finally, Fig. 15 summarises the results obtained for all scenarios considered in terms of Available Electric Energy Flexibility (AEEF) and Specific Cost (SC). The case with a low DR activation threshold ($\beta_{DR} = 0$) exhibits the highest energy flexibility potential, since DR is triggered more times over the day and for a prolonged duration. However, this comes at the cost of higher SC, indicating a major economic drawback. On the other hand, the scenario with a high DR activation threshold ($\beta_{DR} = 2$) achieves the lowest SC, making it the most cost-effective configuration despite having a lower AEEF compared to the previous one. Furthermore, while increasing TES volume generally improves cost stability, excessive DR activation thresholds drive up DR operational expenses, requiring a careful balance between economic feasibility and

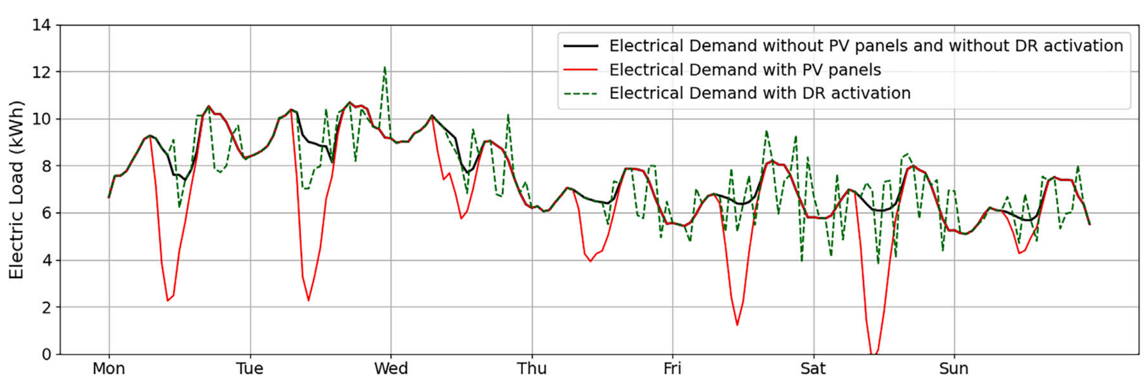

Fig. 13. PV panels share on the electrical consumption (Scenario A).

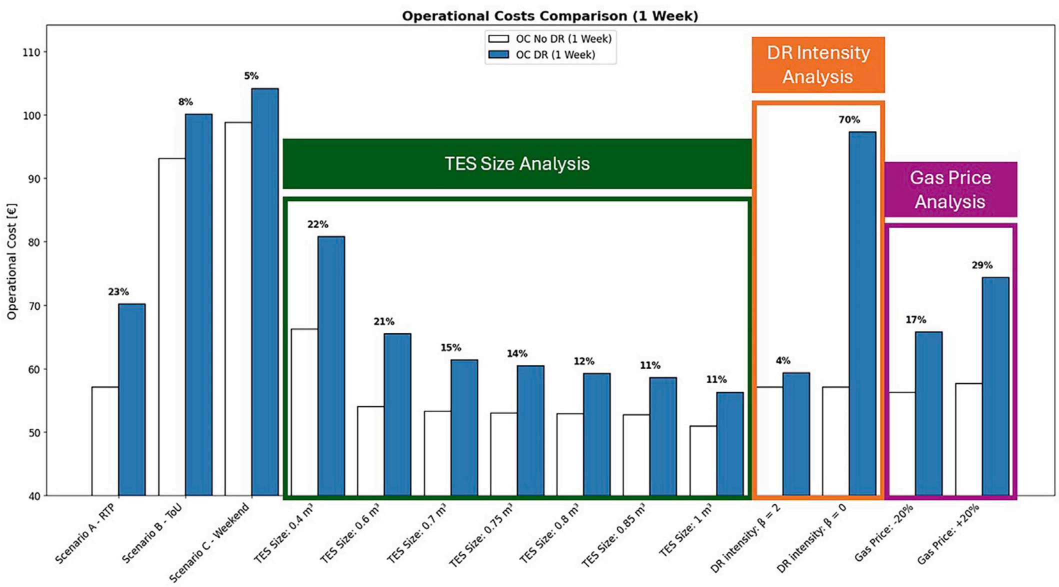

Fig. 14. Heatmaps of the operational costs over a representative winter week, reported both without and with demand response. The results include the three reference electricity tariff schemes (RTP, ToU, and Weekend) as well as the sensitivity analysis carried out from Scenario A (RTP), in which the thermal energy storage size, the demand response intensity (β_{DR}), and the natural gas price were varied.

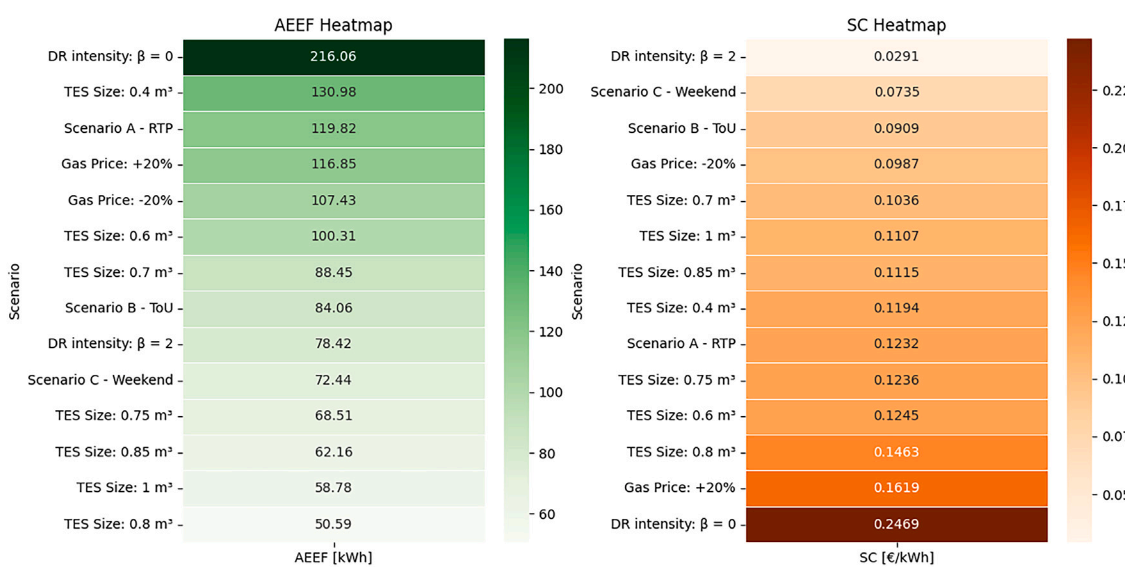

Fig. 15. Heatmaps illustrating the Flexibility Specific Cost and the Available Electric Energy Flexibility over a representative winter week. Results are reported for the three reference price schemes (RTP, ToU, and Weekend). Moreover, the sensitivity analysis was performed starting from Scenario A (RTP) by varying the thermal energy storage size, the demand response intensity (β_{DR}), and the natural gas price.

energy efficiency. Generally, different TES volumes and DR strategies lead to varied trade-offs between efficiency and cost.

4. Conclusion

This research aimed at evaluating both the flexibility potential and the marginal cost of flexibility for a group of buildings. Understanding and quantifying flexibility is essential to enable buildings to participate in energy flexibility markets by providing services that support grid stability. Buildings with flexible energy systems can shift or modulate their loads-either increasing or decreasing consumption-based on external signals. The case study analysed consists of a condominium located in Dublin (Ireland), equipped with a hybrid energy system composed of a gas boiler, a heat pump, photovoltaic panels, and a thermal energy storage unit. To manage the building energy consumption, an energy management system with a smart control algorithm was developed with the objective of minimising the operational cost, considering the contribution of each energy source in meeting both the thermal and electrical demands.

The demand response approach adopted in this work is price-based and reacts to market signals, which are intrinsically linked to the real-time conditions of the electrical grid, such as congestion or peaks in demand. Initially, different electricity tariffs were compared to assess their impact on DR behaviour. Results showed that a tariff scenario based on Real-Time Pricing provides the highest energy flexibility potential and was selected for the subsequent analyses.

Furthermore, the effect of different DR strategies was evaluated by varying the threshold used to activate the response based on electricity prices. The main results showed that with a lower price threshold, which led to the DR being triggered more often and for a prolonged duration, higher AEEF can be achieved (up to about 216 kWh). However this scenario also leads to higher SC (about 0.247 €/kWh), indicating a high flexibility potential but also a significant cost. Conversely, a higher price threshold for DR activation results in lower AEEF (about 78 kWh) and lower SC values (0.029 €/kWh).

Then, the study investigated the impact of DR under different TES volume configurations to determine the most effective size in terms of available energy flexibility potential (AEEF) and specific cost of flexibility (SC). The optimal configuration was found to be a TES volume of 0.5 m^3, which resulted in an AEEF of 119 kWh over one winter week with an SC of 0.123 €/kWh.

The novelty of this work lies in the explicit analysis of the role of thermal energy storage and the separate treatment of the building electrical and thermal energy demands, allowing for a more detailed and accurate modelling approach. Furthermore, the study extends its scope by evaluating the flexibility potential of four buildings connected to a shared energy system. Although the buildings are characterised by the same load profile, their aggregation is explicitly modelled to reflect the operational perspective of an energy aggregator. This approach is fundamental, since flexibility markets are typically accessed through aggregated resources rather than individual buildings. By adopting the aggregator's viewpoint, the analysis provides valuable insights into how collective demand can be mobilised and traded as a single, competitive entity in flexibility markets. Additionally, the integration of renewable energy sources (i.e., photovoltaic systems) reflects the growing penetration of decentralised power generation, highlighting their impact on demand profiles and grid interactions.

Future perspectives include the implementation of different types of DR, such as those responding to technical signals from the grid (e.g., frequency, voltage, or power) and not only price-based triggers. Moreover, this methodology could be extended to different building archetypes to assess the flexibility potential of entire communities. In such a context, the aggregation of multiple buildings could provide significant environmental benefits and have greater influence in the energy market due to their aggregated flexibility capacity.

CRediT authorship contribution statement

Annalisa Bringiotti: Writing – review & editing, Writing – original draft, Validation, Software, Investigation, Formal analysis, Conceptualization. **Fabiano Pallonetto:** Writing – review & editing, Validation, Software, Methodology, Funding acquisition, Conceptualization. **Mattia De Rosa:** Writing – review & editing, Writing – original draft, Validation, Supervision, Methodology, Investigation, Funding acquisition, Formal analysis, Conceptualization.

Declaration of competing interest

The authors declare the following financial interests/personal relationships that may be considered as potential competing interests:

Mattia De Rosa reports that financial support was provided by European Union. If there are other authors, they declare that they have no known competing financial interests or personal relationships that could have appeared to influence the work reported in this paper.

Acknowledgment

M. De Rosa acknowledges the financial support from the European Union - Next Generation EU, Mission 4 Component 1 under PRIN2022 funded by the Italian Ministry of University and Research (MUR), CUP I53C24002620006, project number 2022XCHWT5.

Data availability

Data will be made available on request.

References

[1] Paris Agreement. Report of the conference of the parties to the united nations framework convention on climate change (21st session, 2015: Paris). retrived december. 2015.
[2] Capizzi F, Das A, Dauwe T, Moorkens I, Juhana R, Tomescu M. Renewable energy in europe—2019. European Environmental Agency-European Topic Centre On Climate Change Mitigation And Energy: Mol, Belgium 2019.
[3] Veum K, Bauknecht D. How to reach the eu renewables target by 2030? an analysis of the governance framework. Energy Policy 2019;127:299–307.
[4] Smith O, Cattell O, Farcot E, O'Dea RD, Hopcraft KI. The effect of renewable energy incorporation on power grid stability and resilience. Science Adv 2022;8:eabj6734.
[5] Plaum F, Ahmadiahangar R, Rosin A, Kilter J. Aggregated demand-side energy flexibility: a comprehensive review on characterization, forecasting and market prospects. Energy Rep 2022;8:9344–62.
[6] Yang S, Gao HO, You F. Demand flexibility and cost-saving potentials via smart building energy management: opportunities in residential space heating across the us. Adv Appl Energy 2024;14:100171.
[7] Söder L, Lund PD, Koduvere H, Bolkesjø TF, Rossebø GH, Rosenlund-Soysal E, Skytte K, Katz J, Blumberga D. A review of demand side flexibility potential in northern europe. Renew Sustain Energy Rev 2018;91:654–64.
[8] Rodríguez-Vilches R, Martín-Martínez F, Sánchez-Miralles A., de la Cámara JRG, Delgado SM. Methodology to assess prosumer participation in European electricity markets. Renewable Sustain Energy Rev 2024;191:114179.
[9] Xiong Z, Wang L, Jiang C, Zhou S, Li Y. Bi-level low-carbon optimal operation model of multi-energy aggregator in energy and flexibility market. IEEE Trans Ind Appl 2025.
[10] Breyer C, Khalili S, Bogdanov D, Ram M, Oyewo AS, Aghahosseini A, Gulagi A, Solomon A, Keiner D, Lopez G, et al. On the history and future of 100 % renewable energy systems research. IEEE Access 2022;10:78176–218.
[11] Mohseni-Gharyehsafa B, Bampoulas A, Finn D, Pallonetto F. Energy flexibility and management software in building clusters: a comprehensive review. Next Energy 2025;8:100250.
[12] Berardi U. A cross-country comparison of the building energy consumptions and their trends. Resour Conserv Recycl 2017;123:230–41.
[13] U. N. E. P (UNEP), U. N. E. P (UNEP). Ipcc, intergovernmental panel on climate change.Climate change 2014 - mitigation of climate change, chapter 9 buildings - 2014. UN General Assembly 1988.
[14] Pierce S, Pallonetto F, De Donatis L, De Rosa M. District energy modelling for decarbonisation strategies development—the case of a university campus. Energy Rep 2024;11:1256–67.
[15] Liu Z, Zhang X, Sun Y, Zhou Y. Advanced controls on energy reliability, flexibility and occupant-centric control for smart and energy-efficient buildings. Energy Build 2023;297:113436.
[16] Pallonetto F, De Rosa M, Finn DP. Environmental and economic benefits of building retrofit measures for the residential sector by utilizing sensor data and advanced calibrated models. Adv Build Energy Res 2022;16:89–117.
[17] Pedram O, Asadi E, Chenari B, Moura P, da Silva MG. A review of methodologies for managing energy flexibility resources in buildings. Energies 2023;16:6111.
[18] Valarezo O, Gómez T, Chaves-Avila JP, Lind L, Correa M, Ziegler DU, Escobar R. Analysis of new flexibility market models in europe. Energies 2021;14:3521.
[19] Pallonetto F, De Rosa M, Finn DP. Impact of intelligent control algorithms on demand response flexibility and thermal comfort in a smart grid ready residential building. Smart Energy 2021;2:100017.
[20] Maturo A, Buonomano A, Athienitis A. Design for energy flexibility in smart buildings through solar based and thermal storage systems: modelling, simulation and control for the system optimization. Energy 2022;260:125024.
[21] Lizana J, Friedrich D, Renaldi R, Chacartegui R. Energy flexible building through smart demand-side management and latent heat storage. Appl Energy 2018;230:471–85.
[22] Song M, Sun W. Applications of thermostatically controlled loads for demand response with the proliferation of variable renewable energy. Front Energy 2021: 1–10.
[23] Liang J, Lu Y, Yin G, Fang Z, Zhuang W, Ren Y, Xu L, Li Y. A distributed integrated control architecture of afs and dyc based on mas for distributed drive electric vehicles. IEEE Trans Veh Technol 2021;70:5565–77.
[24] Liang W, Li H, Zhan S, Chong A, Hong T. Energy flexibility quantification of a tropical net-zero office building using physically consistent neural network-based model predictive control. Adv Appl Energy 2024;14:100167.
[25] D'Ettorre F, De Rosa M, Conti P, Schito E, Testi D, Finn DP. Economic assessment of flexibility offered by an optimally controlled hybrid heat pump generator: a case study for residential building. Energy Procedia 2018;148:1222–9.
[26] Fitzpatrick P, D'Ettorre F, De Rosa M, Yadack M, Eicker U, Finn DP. Influence of electricity prices on energy flexibility of integrated hybrid heat pump and thermal storage systems in a residential building. Energy And Buildings 2020;223:110142.
[27] Hao CH, Jr PKW, Wang J, Abudu H, Dogah KE, Okorie DI, Opoku EEO. Dynamic pricing in consumer-centric electricity markets: a systematic review and thematic analysis. Energy Strateg Rev 2024;52:101349.
[28] Putrayudha SA, Kang EC, Evgueniy E, Libing Y, Lee EJ. A study of photovoltaic/thermal (pvt)-ground source heat pump hybrid system by using fuzzy logic control. Appl Therm Eng 2015;89:578–86.

[29] Junker RG, Azar AG, Lopes RA, Lindberg KB, Reynders G, Relan R, Madsen H. Characterizing the energy flexibility of buildings and districts. Appl Energy 2018;225:175–82.
[30] Saberi-Derakhtenjani A, Barbosa JD, Rodriguez-Ubinas E. Energy flexibility strategies for buildings in hot climates: a case study for dubai. Buildings 2024;14:3008.
[31] Yang P, Jiang H, Liu C, Kang L, Wang C. Coordinated optimization scheduling operation of integrated energy system considering demand response and carbon trading mechanism. Int J Electr Power Energy Syst 2023;147:108902.
[32] Neu O, Oxizidis S, Flynn D, Pallonetto F, Finn D. High resolution space-time data: methodology for residential building simulation modelling, In: Wurtz, E(ed.). Proceedings of BS2013: 13th Conference of International Building Performance Simulation Association, Chambéry, France, August 26-28; International Building Performance Simulation Association (IBPSA); 2013.
[33] Cui D, Liang S, Wang D. Observed and projected changes in global climate zones based on köppen climate classification. Wiley Interdiscip Rev Clim Change 2021;12:e701.
[34] Lohmann U, Sausen R, Bengtsson L, Cubasch U, Perlwitz J, Roeckner E. The köppen climate classification as a diagnostic tool for general circulation models. Clim Res 1993:177–93.
[35] Crawley DB, Lawrie LK, Pedersen CO, Winkelmann FC. Energy plus: energy simulation program. Ashrae J 2000;42:49–56.
[36] Thorvaldsen KE, Korpås M, Farahmand H. Long-term value of flexibility from flexible assets in building operation. Int J Electr Power Energy Syst 2022;138:107811.
[37] Marino DL, Amarasinghe K, Manic M. Building energy load forecasting using deep neural networks, In: IECON 2016-42nd annual conference of the IEEE industrial electronics society; IEEE; 2016. p. 7046–51.
[38] Bagarella G, Lazzarin R, Noro M. Sizing strategy of on–off and modulating heat pump systems based on annual energy analysis. Int J Refrig 2016;65:183–93.
[39] Perrella S, Bisegna F, Bevilacqua P, Cirone D, Bruno R. Solar-assisted heat pump with electric and thermal storage: the role of appropriate control strategies for the exploitation of the solar source. Buildings 2024;14.
[40] D'Ettorre F, De Rosa M, Conti P, Testi D, Finn D. Mapping the energy flexibility potential of single buildings equipped with optimally-controlled heat pump, gas boilers and thermal storage. Sustain Cities Soc 2019;50:101689.
[41] Pallonetto F, Oxizidis S, Milano F, Finn D. The effect of time-of-use tariffs on the demand response flexibility of an all-electric smart-grid-ready dwelling. Energy And Buildings 2016;128:56–67.
[42] Scarpa F, Tagliafico LA, Bianco V. Inverse cycles modeling without refrigerant property specification. Int J Refrig 2013;36:1716–29.
[43] Akau R, Schoenhals R. The second law efficiency of a heat pump system. Energy 1980;5:853–63.
[44] Badescu V. First and second law analysis of a solar assisted heat pump based heating system. Energy Convers Manag 2002;43:2539–52.
[45] Fux SF, Benz MJ, Guzzella L. Economic and environmental aspects of the component sizing for a stand-alone building energy system: a case study. Renew. Energy 2013;55:438–47.
[46] Renaldi R, Kiprakis A, Friedrich D. An optimisation framework for thermal energy storage integration in a residential heat pump heating system. Appl Energy 2017;186:520–9. Sustainable Thermal Energy Management (SusTEM2015).
[47] Henze GP, Felsmann C, Knabe G. Evaluation of optimal control for active and passive building thermal storage. Int J Therm Sci 2004;43:173–83.
[48] Mawire A. Experimental and simulated thermal stratification evaluation of an oil storage tank subjected to heat losses during charging. Appl Energy 2013;108:459–65.
[49] Vérez D, Borri E, Crespo A, Zsembinszki G, Dawoud B, Cabeza LF. Experimental study of a small-size vacuum insulated water tank for building applications. Sustainability 2021;13.
[50] Kalaiselvam S, Parameshwaran R. Thermal energy storage technologies for sustainability: systems design, assessment and applications. Elsevier; 2014.
[51] Yang C, Meng C, Zhou K. Residential electricity pricing in China: the context of price-based demand response. Renew Sustain Energy Rev 2018;81:2870–8.
[52] Fischer D, Lindberg KB, Madani H, Wittwer C. Impact of pv and variable prices on optimal system sizing for heat pumps and thermal storage. Energy And Buildings 2016;128:723–33.
[53] Lobontiu N. Chapter 5 - fluid and thermal systems. In Lobontiu N, editor. System dynamics for engineering students (second edition). Boston: Academic Press; 2018. pp. 213–72. https://doi.org/10.1016/B978-0-12-804559-6.00005-1. https://www.sciencedirect.com/science/article/pii/B9780128045596000051.
[54] Diab I, Damianakis N, Chandra-Mouli GR, Bauer P. A shared pv system for transportation and residential loads to reduce curtailment and the need for storage systems. Appl Energy 2024;353:122131.
[55] Lazzarin R, Noro M. Photovoltaic/Thermal (pv/t)/ground dual source heat pump: optimum energy and economic sizing based on performance analysis. Energy And Buildings 2020;211:109800.
[56] Maleki SAM, Hizam H, Gomes C. Estimation of hourly, daily and monthly global solar radiation on inclined surfaces: models re-visited. Energies 2017;10:134.
[57] Jacobson MZ, Jadhav V. World estimates of pv optimal tilt angles and ratios of sunlight incident upon tilted and tracked pv panels relative to horizontal panels. Solar Energy 2018;169:55–66.
[58] Dubey S, Sarvaiya JN, Seshadri B. Temperature dependent photovoltaic (pv) efficiency and its effect on pv production in the world–a review. Energy Procedia 2013;33:311–21.
[59] Peng Z, Herfatmanesh MR, Liu Y. Cooled solar pv panels for output energy efficiency optimisation. Energy Convers Manag 2017;150:949–55.
[60] ENTSO-E. Day-ahead market prices - pt60m. 2023. https://newtransparency.entsoe.eu/market/prices/dayAhead/PT60M. [Accessed: 2024-10-22].
[61] Bord Gáis Energy. Our plans - electricity tariffs. 2024. https://www.bordgaisenergy.ie/home/our-plans?fuelType=ELECTRICITY&smartMeter=SMARTMETER_NO. [Accessed: 2024-Oct-22].
[62] Eurostat. Electricity prices for household consumers - bi-annual data (from 2007 onwards). 2024. https://ec.europa.eu/eurostat/databrowser/view/ten00118/default/table?lang=en. [Accessed: 2024-Oct-22].
[63] Zhu Z, Lambotharan S, Chin WH, Fan Z. A game theoretic optimization framework for home demand management incorporating local energy resources. IEEE Trans Ind Informatics 2015;11:353–62.
[64] Yang X, Zhang Y, Zhao B, Huang F, Chen Y, Ren S. Optimal energy flow control strategy for a residential energy local network combined with demand-side management and real-time pricing. Energy And Buildings 2017;150:177–88.
[65] Spivak DA. Optimization, evaluation, and characterization of molecularly imprinted polymers. Adv Drug Deliv Rev 2005;57:1779–94.
[66] Huang W, Zhang N, Kang C, Li M, Huo M. From demand response to integrated demand response: review and prospect of research and application. Prot Control Mod Power Syst 2019;4:1–13.
[67] Yan X, Ozturk Y, Hu Z, Song Y. A review on price-driven residential demand response. Renew Sustain Energy Rev 2018;96:411–9.
[68] Balasubramanian C, Singh RLR. Iot based energy management in smart grid under price based demand response based on hybrid fho-rernn approach. Appl Energy 2024;361:122851.
[69] Li H, Johra H, Pereira FDA, Hong T, Le Dréau J, Maturo A, Wei M, Liu Y, Saberi-Derakhtenjani A, Nagy Z, et al. Data-driven key performance indicators and datasets for building energy flexibility: a review and perspectives. Appl Energy 2023;343:121217.
[70] Milano F, Ortega A. A method for evaluating frequency regulation in an electrical grid–part i: theory. IEEE Trans Power Syst 2020;36:183–93.
[71] Schwarzmayr P, Birkelbach F, Walter H, Hofmann R. Standby efficiency and thermocline degradation of a packed bed thermal energy storage: an experimental study. Appl Energy 2023;337:120917.